

Buckling of Axisymmetric Imperfect Circular Cylindrical Shells under Axial Compression

R. C. TENNYSON* AND D. B. MUGGERIDGE†
University of Toronto, Toronto, Ontario, Canada

Circular cylindrical shells containing axisymmetric imperfections in shape described by a simple trigonometric function have been tested under axial compressive loading. Various values of imperfection amplitude and wavelength were considered and the results compared with Koiter's extended theory. Numerical calculations were also made using an exact model formulation including the effects of end constraint and cylinder geometry. For each shell configuration analysed, the exact model results agreed with Koiter's extended theory within a few percent. In general, theory and experiment agreed within 10%. It was also observed that a critical axisymmetric wavelength existed which yielded a minimum buckling load for a given value of imperfection amplitude, consistent with the predictions of Koiter's extended theory. Only in the limiting case of imperfection amplitude approaching zero does the critical wavelength correspond to the classical axisymmetric buckling mode of a perfect shell.

Nomenclature

b	$=(4\rho^4 + 1)/(4\rho^4 + 1 - 4\lambda\rho^2)$
c	$=[3(1 - \nu^2)]^{1/2}$
E	modulus of elasticity
\bar{F}	Airy stress function
F	$=2c\bar{F}/El^3$
h	$=t/l$
K	$=p/q_0$
L	shell length
l_x	$=L/m = \pi R/2p$, axial half-wave length
m, n	number of half-waves and waves in the axial and circumferential directions, respectively
$-N$	applied compressive load per unit length
p	$=m\pi R/2L$
q_0	$=(R/t)^{1/2}[12(1 - \nu^2)]^{1/4}$, the classical axisymmetric buckling mode wave number
R	shell radius measured to median surface
t	shell wall thickness
\bar{t}	average shell wall thickness
$\bar{u}, \bar{v}, \bar{w}$	displacements measured in the axial, circumferential and radial directions, respectively
u, v, w	$=\bar{u}/\bar{t}, \bar{v}/\bar{t}, \bar{w}/\bar{t}$, respectively
$\bar{w}(x)$	$=(-\delta/2\bar{t})\cos(\pi\bar{x}/l_x)$, deviation of median surface
\bar{x}, \bar{y}	axial and circumferential coordinates, respectively
x, y	$=\bar{x}/L, \bar{y}/L$, respectively
Z	$=L^2(1 - \nu^2)^{1/2}/Rt$
β	$=nL/R$
δ	peak axisymmetric imperfection amplitude
$\lambda, \lambda^*, \lambda_e$	$=\sigma_e/\sigma_{cl}, \sigma_{er}/\sigma_{cl}, \sigma_e/\sigma_{cl}$, respectively
μ	maximum deviation of median surface/average shell wall thickness
ν	Poisson's ratio
ρ	$=p(t/Rc)^{1/2}$
σ_{cl}	$=El/Rc$, classical compressive buckling stress for a perfect circular cylindrical shell
σ_k	cylinder buckling stress corresponding to Koiter's extended theory
σ_{er}	critical cylinder buckling stress observed experimentally
σ_e	cylinder buckling stress as computed from exact model formulation
τ	$=n(t/Rc)^{1/2}$

Subscripts

avg	average
cl	classical

Received April 4, 1969. The authors wish to acknowledge the financial assistance of the National Research Council of Canada (Grant A-2783) and of NASA [Grant NGR 52-026-(011, Supplement 1] which made this research possible. The numerical computations were supported by NASA Grant NGL 22-007-012 with Harvard University.

* Associate Professor, Institute for Aerospace Studies. Member AIAA.

† Research Assistant, Institute for Aerospace Studies.

cr	= critical
e	= refers to exact model theory
k	= refers to Koiter's theory
0	= prebuckling axisymmetric solution

I. Introduction

IT is now generally recognized that imperfections in shape play the dominant role in reducing the buckling load of a circular cylindrical shell under axial compressive loading. In previous work Tennyson¹ has shown that geometrically "near-perfect" circular cylinders buckle within a few percent of the reduced classical value taking into account the effect of end constraints. Due to the prebuckling deformations introduced by the boundary conditions, the edge constraint can also be regarded as a particular type of axisymmetric imperfection. However, in most cases of practical interest, clamped edge support is usually present and the load reduction based on the classical value is nominally 9 ~ 10%.

Theoretical analyses²⁻⁷ of the effect of imperfections on the buckling behavior of cylinders have clearly demonstrated that relatively small imperfection amplitudes can drastically reduce the critical load of the shell. Despite the substantial theory available, few experimental data⁸⁻¹⁰ exist describing the effects of specific imperfections in shape in reducing the static buckling load. Consequently, it was of particular interest to determine the buckling load reduction caused by an initial axisymmetric imperfection in shape defined by a simple trigonometric function.^{2,3} In his "special theory,"³ which was formulated neglecting end constraints, Koiter verified the asymptotic relationship presented earlier in his more "general theory"² for the limiting case of the axisymmetric imperfection amplitude approaching zero. Moreover, Koiter was able to derive an equation that predicted the effects of finite imperfections on the buckling load for wavelengths equal to the classical axisymmetric buckling mode of a perfect shell.

This paper describes an investigation of the influence of axisymmetric imperfection profiles of varying wavelength and amplitude on the buckling behavior of circular cylindrical shells subjected to axial compression. Using Koiter's theory,³ it was possible to extend his analysis for arbitrary values of imperfection wavelength and amplitude, the results of which are contained in this paper. In order to test Koiter's extended theory, photoelastic plastic circular cylindrical shells containing an axisymmetric imperfection in shape were manufactured by the spin-casting technique¹ and subjected to axial compression. For comparison purposes, numerical buckling load calculations were performed by Hutchinson¹¹ based on an exact analytical model in which the effects of a clamped end constraint and the specific geometrical configuration of the cylinders were taken into account.

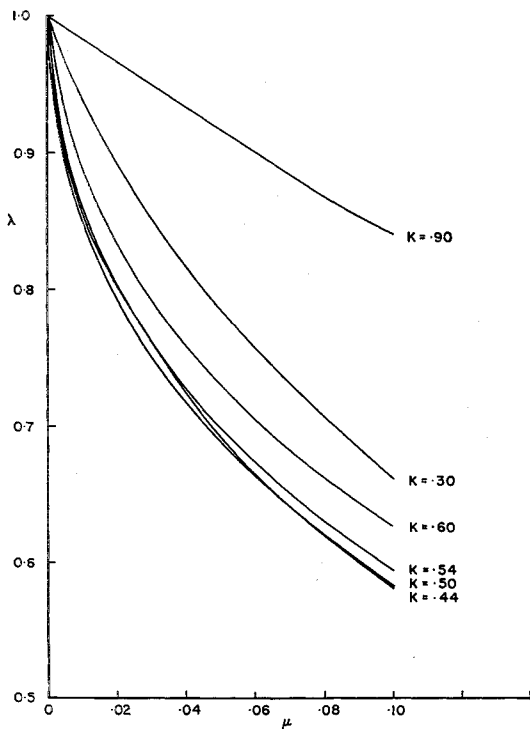


Fig. 1 Buckling load ratio vs axisymmetric imperfection amplitude for varying values of axial wave number.

II. Basic Equations

Koiter's Extended Theory

The problem of determining the effect of axisymmetric imperfections in shape on the buckling behavior of a circular cylindrical shell subjected to axial compression was first analysed by Koiter.² In his general theory, Koiter considered an imperfection wavelength equal to the classical axisymmetric buckling mode (in terms of the wave number used in this paper, this corresponds to $K = \frac{1}{2}$) and an asymptotic solution was obtained for small values of the imperfection amplitude μ . Subsequently, Koiter formulated a special theory³ and derived a first approximation to the critical buckling load solution for finite values of the imperfection amplitude which, for $K = \frac{1}{2}$ and $\mu \rightarrow 0$, verified the results of his former general theory. In each case, a constant thickness cylinder containing an initial axisymmetric imperfection profile having the form $\bar{w}(\bar{x}) = -\mu t \cos(2p\bar{x}/R)$ was assumed, and the prebuckling deformations due to edge constraint were neglected. From Koiter's special theory using a Galerkin procedure, an upper bound to the critical buckling load parameter λ can be found from the following eigen value equation:

$$(\rho^2 + \tau^2)^2 + 4\rho^4(\rho^2 + \tau^2)^{-2} - 4\lambda\rho^2 - 2c\mu\tau^2[b - 1 + 8b\rho^4(\rho^2 + \tau^2)^{-2}] + 16(c\mu)^2b^2\rho^4\tau^4[(\rho^2 + \tau^2)^{-2} + (9\rho^2 + \tau^2)^{-2}] = 0 \quad (1)$$

where ρ is a nondimensional axial wave number and τ is a free parameter associated with the asymmetric bifurcation mode. Koiter solved Eq. (1) for the particular case when $\rho^2 = \frac{1}{2}$, which corresponds to the axisymmetric imperfection wavelength equal to the classical axisymmetric buckling mode of the perfect circular cylindrical shell, that is,

$$2p = q_0 = [12(1 - \nu^2)]^{1/4}(R/t)^{1/2} \quad (2)$$

As noted by Koiter,³ Eq. (1) can also be solved for various values of the imperfection wavelength and amplitude. Consequently, using the following definitions:

$$p = Kq_0 \quad (3)$$

$$\rho^2 = 2K^2 \quad (4)$$

Eq. (1) can be rewritten in the form

$$A_1\lambda^3 + A_2\lambda^2 + A_3\lambda + A_4 = 0 \quad (5)$$

where

$$\begin{aligned} A_1 &= -512K^6Q^2 \\ A_2 &= 64K^4Q^4 + 1024K^8 + 128K^4BQ^2 + 128c\mu\tau^2K^4Q^2 \\ A_3 &= -16K^2BQ^4 - 256K^6B - 8K^2Q^2B^2 - \\ &\quad 16c\mu\tau^2K^2Q^2B + 512c\mu\tau^2K^6B \\ A_4 &= Q^4B^2 + 16K^4B^2 - 64c\mu\tau^2K^4B^2 + \\ &\quad 64(c\mu)^2K^4Q^2\tau^4B^2H \end{aligned} \quad (6)$$

$$Q = 2K^2 + \tau^2, \quad B = 16K^4 + 1$$

$$H = 1/Q^2 + 1/(18K^2 + \tau^2)^2$$

Thus, for given values of K and μ , a minimum value of λ can be determined from Eq. (5) by varying the circumferential wave number parameter τ . Figures 1 and 2 show the solutions obtained for $0 \leq \mu \leq 0.1$ and $0 \leq \mu \leq 1.0$, respectively (taking $\nu = 0.4$ as is appropriate for the shells tested). The envelope defining the lower bound of minimum λ vs μ for all values of K is plotted in Fig. 3, which lies somewhat lower than Koiter's results³ for $K = \frac{1}{2}$. Only as $\mu \rightarrow 0$ (i.e., the asymptotic solution) does $K = \frac{1}{2}$ yield the minimum buckling load as demonstrated in Fig. 4. It is quite clear from the analysis that the critical imperfection wavelength leading to a minimum buckling load increases for increasing values of the imperfection amplitude. This analysis is limited, however, by the conditions on the wave numbers (m, n must be large) and by the initial buckling mode assumed by Koiter.³

Exact Model Formulation†

Because of the technique used to fabricate the photoelastic plastic test cylinders, the imperfection was cut only on the inside wall of the shell, thus resulting in axisymmetric thickness

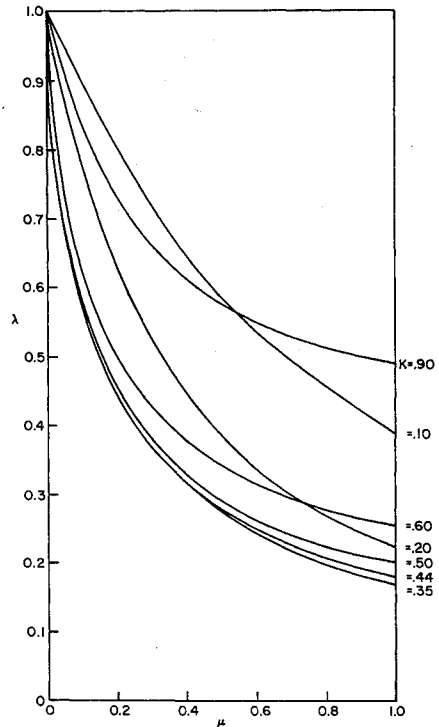


Fig. 2 Buckling load ratio vs axisymmetric imperfection amplitude for varying values of axial wave number.

† The authors wish to acknowledge gratefully that this analysis was performed for comparison purposes by J. W. Hutchinson, Harvard University.

and median surface profiles given by (refer to Fig. 5)

$$\begin{aligned} t(\bar{x}) &= \bar{t}[1 + (\delta/\bar{t}) \cos(\pi\bar{x}/l_x)] \\ \tilde{w}(\bar{x}) &= -(\delta/2) \cos(\pi\bar{x}/l_x) \end{aligned} \quad (7)$$

Hence, it was necessary to determine the extent to which the thickness variation in combination with the prebuckling deformations due to the clamped end constraint would reduce the buckling load estimates based on Koiter's extended theory. The following nondimensional form⁸ of the equilibrium and compatibility equations was derived by Hutchinson¹¹:

$$\begin{aligned} &[h^3(w_{,xx} + \nu w_{,yy})]_{,xx} + h^3(w_{,yyy} + \nu w_{,xxyy}) + \\ &2(1 - \nu)(h^3 w_{,xyy})_{,x} + 2(3)^{1/2} Z F_{,xx} = \\ &2c[F_{,yy}(w_{,xx} + \tilde{w}_{,xx}) + F_{,xx}w_{,yy} - 2F_{,xy}w_{,xy}] \quad (8) \\ &(1/h)(F_{,yyy} - \nu F_{,xxy}) + [(1/h)(F_{,xx} - \nu F_{,yy})]_{,xx} + \\ &2(1 + \nu)[(1/h)F_{,xyy}]_{,x} - 2(3)^{1/2} Z w_{,xx} = \\ &2c[-w_{,yy}(w_{,xx} + \tilde{w}_{,xx}) + w_{,xy}^2] \quad (9) \end{aligned}$$

When $h = \text{const}$, Eqs. (8) and (9) reduce to those used by Koiter.³

The prebuckling axisymmetric solution can be obtained from Eqs. (8) and (9), noting that $F_{0,yy} = -N$,

$$(h^3 w_{0,xx})_{,xx} + 2(3)^{1/2} Z F_{0,xx} + 2cN(w_{0,xx} + \tilde{w}_{,xx}) = 0 \quad (10)$$

$$[(1/h)F_{0,xx}]_{,xx} - 2(3)^{1/2} Z w_{0,xx} + \nu N(1/h)_{,xx} = 0 \quad (11)$$

For the clamped end constraint appropriate to the cylinder configuration being studied, the following boundary conditions are applicable:

$$\begin{aligned} w_0 &= w_0 = w_{0,x} = 0 \text{ at } x = 0, 1 \\ u_0 &= 0 \text{ at } x = 0 \\ u_0 &= u_0(N) \text{ at } x = 1 \end{aligned} \quad (12)$$

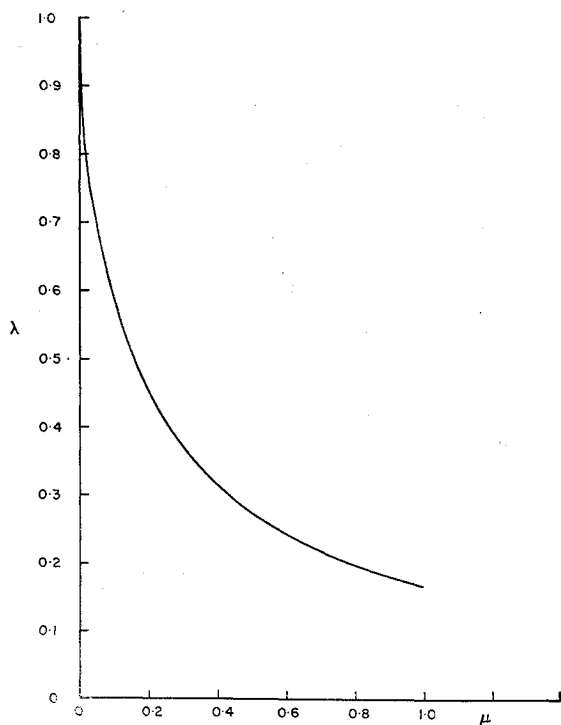


Fig. 3 Envelope of minimum buckling load ratio vs axisymmetric imperfection amplitude.

⁸ Subscripts following a comma indicate differentiation with respect to the variables shown.

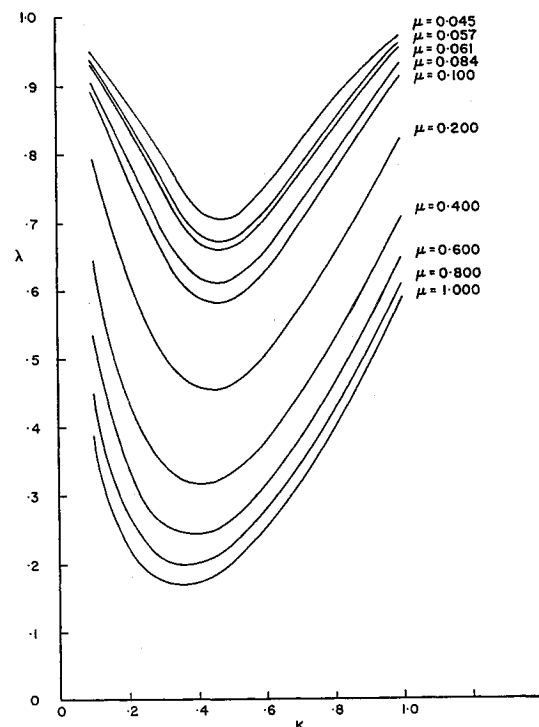


Fig. 4 Buckling load ratio vs axial wave number for varying values of axisymmetric imperfection amplitude.

Hence, Eq. (11) yields

$$F_{0,xx} = -\nu N + 2(3)^{1/2} Z h w_0 \quad (13)$$

which, when substituted into Eq. (10), gives

$$\begin{aligned} (h^3 w_{0,xx})_{,xx} + 2cN(w_{0,xx} + \tilde{w}_{,xx}) + 12Z^2 h w_0 - \\ 2(3)^{1/2} Z \nu N = 0 \quad (14) \end{aligned}$$

The solution of Eqs. (13) and (14) yields the prebuckling values F_0 , w_0 necessary for the complete buckling solution of Eqs. (8) and (9). It is assumed that the form of F and w which will satisfy the equilibrium and compatibility equations at the inception of buckling is given by

$$\begin{aligned} w &= w_0 + \epsilon w_1 \\ F &= F_0 + \epsilon F_1 \end{aligned} \quad (15)$$

where

$$\begin{aligned} w_1 &= w_1(x) \cos \beta y \\ F_1 &= F_1(x) \cos \beta y \end{aligned} \quad (16)$$

Substituting Eqs. (15) and (16) into Eqs. (8) and (9) and

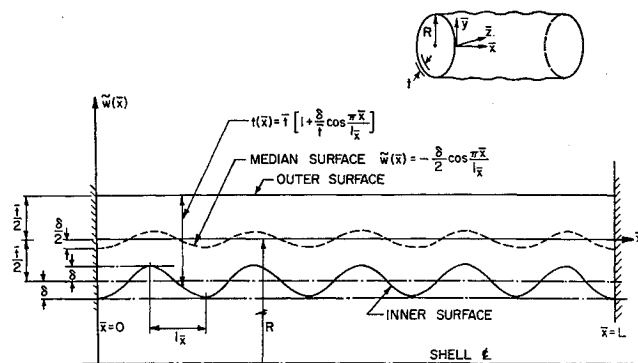


Fig. 5 Circular cylinder with axisymmetric shape imperfection.

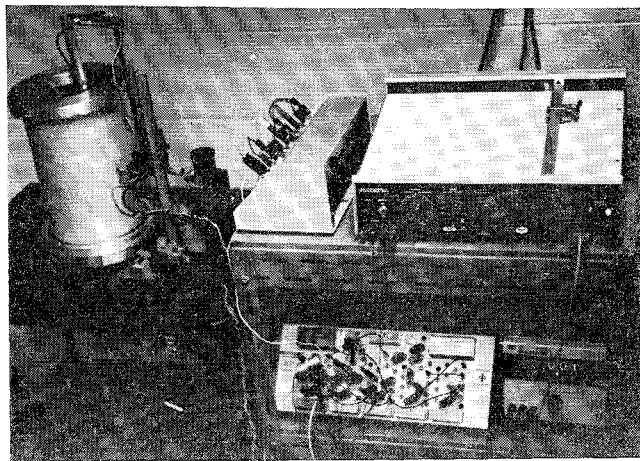


Fig. 6 Apparatus for measuring shell wall profile.

retaining only first-order terms in ϵ gives

$$\begin{aligned}
 & [h^3(w_{1,xx} - \nu\beta^2 w_1)],_{xx} + h^3(\beta^4 w_1 - \nu\beta^2 w_{1,xx}) - \\
 & 2(1-\nu)\beta^2(h^3 w_{1,x}),_x + 2(3)^{1/2} Z F_{1,xx} + \\
 & 2cN w_{1,xx} = 2c[-\beta^2 F_1(w_{0,xx} + \tilde{w}_{xx}) - \beta^2 w_{F,0,xx}] \quad (17)
 \end{aligned}$$

$$1/h(\beta^4 F_1 + \nu \beta^2 F_{1,xx}) + [1/h(F_{1,xx} + \nu \beta^2 F_1)]_{xx} = 2(1 +$$

$$v) \beta^2 [1/hE, \ldots] = 2(3)^{1/2} Z w_1 = 2c \beta^2 w_1 (w_{0,xx} + \tilde{w}_{xx}) \quad (18)$$

with the appropriate boundary conditions at the shell ends defined by

$$u_1 = v_1 = w_1 = w_{1,x} = 0 \quad \text{at } x = 0, 1 \quad (19)$$

Equations (13, 14, 17, and 18) were solved numerically by Hutchinson,¹¹ and the results are discussed later in conjunction with the experimental data. Illustrations of the numerical technique employed to solve these equations can be found in Ref. 13.

III. Experiment—Fabrication and Test Procedure

In the experimental programs conducted to date, all circular cylindrical shells have been manufactured from a photoelastic plastic using the spin-casting technique.¹ Initially, a geometrically near-perfect shell was cast and the inner wall

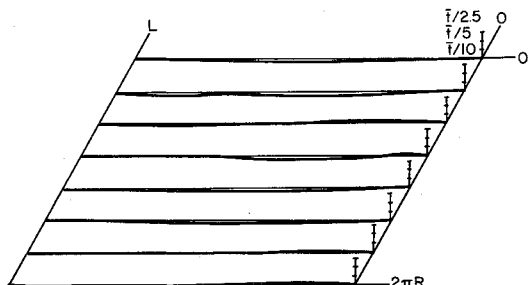


Fig. 7a) Profile of the median surface on a near-perfect circular cylindrical shell containing random imperfections.

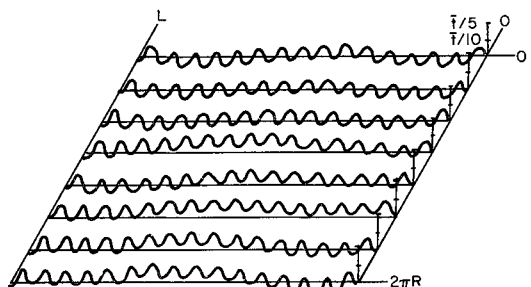


Fig. 7b) Profile of the median surface of a circular cylindrical shell containing axisymmetric imperfections in shape.

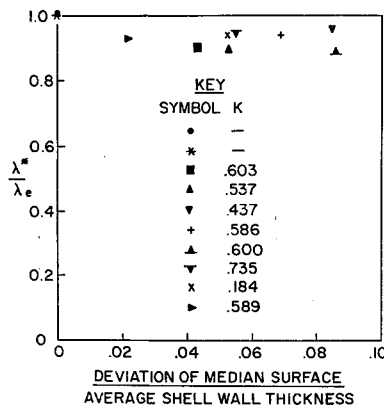


Fig. 8 Comparison of axisymmetric imperfect shell buckling loads with Koiter's extended theory.

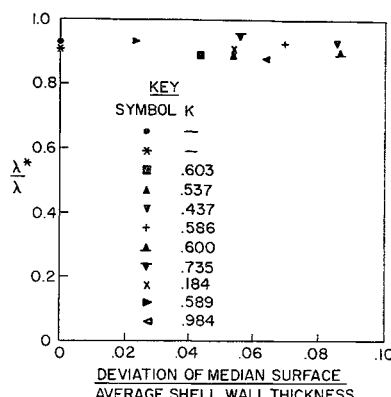
machined to a prescribed profile. In order to construct the axisymmetric imperfection wave form, a metal template containing the desired wavelength and amplitude was used in conjunction with a hydraulic tracer-tool apparatus. By cutting the imperfection profile only on the inner surface, the shell was easily separated from the casting form. After removing the cylinder, thickness measurements were made at discrete points around the circumference at both ends. Machined aluminum end plates were then attached to the test cylinder to provide the clamped edge restraint. Each shell was subsequently positioned in a rotation apparatus, as shown in Fig. 6, and the inner, outer, and median surface profiles were determined using low-pressure, linear contacting displacement transducers with their outputs recorded on an x - y plotter. Figure 7a illustrates median surface profiles obtained from a geometrically near-perfect shell and Fig. 7b illustrates profiles from a shell containing the axisymmetric imperfection in shape. Although a contact measuring system does not represent the optimum technique, it was deemed acceptable particularly for the shell wall thicknesses involved and the very low spring stiffness of each probe. The measured thicknesses at the shell ends served as a reference for determining absolute variations along each generator.

The final stage of the test procedure involved the proper alignment of the cylinder in an electrically driven, four-screw compression machine. Uniformity of the applied stress was easily checked by examining photoelastically the membrane stress distribution around the circumference of the cylinder and finally, by noting the postbuckled configuration of the cylinder. Complete circumferential buckling centrally located in the shell attested to the uniformity of the load distribution. Since each shell buckled elastically and repeatedly at the same load, it was possible to employ high-speed framing photography to analyse the inception of buckling using the method of isoclinics.¹² Although some results are available, they will not be included in this paper.

To serve as reference shells, two geometrically near-perfect cylinders were tested in axial compression to determine the modulus of elasticity of the epoxy plastic used in each test series, and, at the same time, to provide a measure of the load

Table 1 Properties of axisymmetric imperfect shells

Fig. 9 Comparison of axisymmetric imperfect shell buckling loads with exact model theory.



reduction due to the clamped end constraint common to each shell. In total, nine cylinders of varying imperfection wavelength and amplitude were studied (refer to Table 1), the results of which are discussed in the next section.

IV. Discussion of Experimental Results

A comparison of the shell buckling data with Koiter's extended theory and the results of the exact model analysis are contained in Figs. 8 and 9, respectively. In each case, the experimental data are within 10% of the predicted values. The remarkable feature of the comparison between Koiter's simple model and the exact formulation is that for the range of imperfection amplitude and axial wave number parameters considered, no significant difference exists between the critical loads. Hence, it appears that the load reduction due to initial shape imperfections is the dominant factor completely overwhelming the effects of thickness variation and end constraint.

To determine the effect of imperfection amplitude on the critical buckling load, three shells were tested having nominally the same axial wave number parameter ($K_{avg} = 0.592$) and varying values of imperfection amplitude. The results are shown in Fig. 10 and a comparison is made with both Koiter's extended theory and the exact model calculations. It was also of interest to determine if a critical axisymmetric imperfection wavelength existed which would yield a minimum buckling load for a given value of imperfection amplitude. Again, three shells were tested having nominally the same imperfection amplitude parameter (≈ 0.054) and varying values of the axial wave number parameter K . As shown in Fig. 11, a critical value of K does indeed exist at which a minimum buckling load is observed, consistent with the results of Koiter's extended theory. It should be noted that in Koiter's original analysis,³ only as $\mu \rightarrow 0$ does this critical value of K approach $\frac{1}{2}$. For finite values of imperfection, the critical value of K must be determined from the extended analysis. The exact model results are also shown in Fig. 11 for comparison purposes and again it is noted that the difference between Koiter's extended theory and experiment is small over the range plotted.

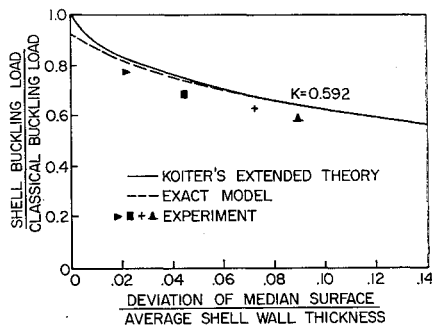


Fig. 10 Critical shell buckling load ratio vs (axisymmetric imperfection amplitude/average shell wall thickness) for a particular value of imperfection wave number.

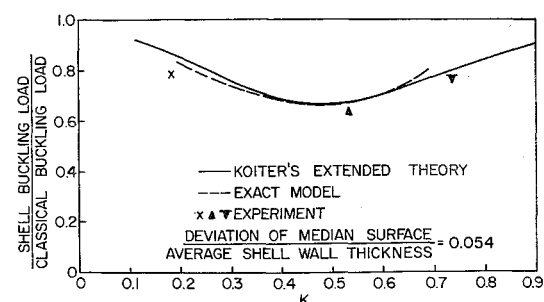


Fig. 11 Critical shell buckling load ratio vs axisymmetric imperfection wave number for a particular value of imperfection amplitude.

V. Conclusions

The experimental results achieved to date constitute the first verification of Koiter's imperfection theory which was extended to include buckling load solutions for a wide range of axisymmetric imperfection wavelengths. In all cases, experimental results and theory agree within 10%. Although it is somewhat surprising that the exact model calculations do not yield critical buckling loads significantly lower than the predictions of Koiter's theory, it is concluded that for the range of parameters considered, the effects of a clamped edge constraint in combination with an arbitrary thickness variation can be neglected, and that very small shape imperfections drastically reduce the buckling load of a circular cylindrical shell in axial compression.

References

- 1 Tennyson, R. C., "An Experimental Investigation of the Buckling of Circular Cylindrical Shells in Axial Compression Using the Photoelastic Technique," Rept. 102, Nov. 1964, Univ. of Toronto Inst. for Aerospace Studies.
- 2 Koiter, W. T., "On the Stability of Elastic Equilibrium" (in Dutch with English summary), Ph.D. thesis, Delft, H. J. Paris, Amsterdam, 1945; also TT F-10, 833, March 1967, NASA.
- 3 Koiter, W. T., "The Effect of Axisymmetric Imperfections on the Buckling of Cylindrical Shells Under Axial Compression," TR 6-90-63-86, Aug. 1963, Lockheed Missiles & Space Co.
- 4 Hutchinson, J., "Axial Buckling of Pressurized Imperfect Cylindrical Shells," AIAA Journal, Vol. 3, No. 8, Aug. 1965, pp. 1461-1466.
- 5 Almroth, B. O., "Influence of Imperfections and Edge Restraint on the Buckling of Axially Compressed Cylinders," CR-432, April 1966, NASA.
- 6 Budiansky, B. and Hutchinson, J. W., "A Survey of Some Buckling Problems," AIAA Journal, Vol. 4, No. 9, Sept. 1966, pp. 1505-1510.
- 7 Dym, C. L. and Hoff, N. J., "Perturbation Solutions for the Buckling Problems of Axially Compressed Thin Cylindrical Shells of Infinite or Finite Length," Journal of Applied Mechanics, Dec. 1968.
- 8 Babcock, C. D. and Sechler, E. E., "The Effect of Initial Imperfections on the Buckling Stress of Cylindrical Shells," TN D-2005, July 1963, NASA.
- 9 Babcock, C. D., "The Influence of a Local Imperfection on the Buckling Load of a Cylindrical Shell Under Axial Compression," SM-68-4, Feb. 1968, Graduate Aeronautical Lab., Calif. Inst. of Technology.
- 10 Arboz, J. and Babcock, C. D., "Experimental Investigation of the Effect of General Imperfections on the Buckling of Cylindrical Shells," SM 68-7, Feb. 1968, Graduate Aeronautical Lab., Calif. Inst. of Technology.
- 11 Hutchinson, J. W., private communication, Harvard University, 1969.
- 12 Tennyson, R. C. and Welles, S. W., "Analysis of the Buckling Process of Circular Cylindrical Shells Under Axial Compression," Rept. 129, Feb. 1968, Univ. of Toronto Institute for Aerospace Studies.
- 13 Budiansky, B. and Radkowsky, P. P., "Numerical Analysis of Unsymmetrical Bending of Shells of Revolution," AIAA Journal, Vol. 1, No. 8, Aug. 1963, pp. 1833-1847.